PLCβ3 mediates cortactin interaction with WAVE2 in MCP1-induced actin polymerization and cell migration

Jagadeesh Janjanam, Giri Kumar Chandaka, Sivareddy Kotla, and Gadiparthi N. Rao
Department of Physiology, University of Tennessee Health Science Center, Memphis, TN 38163

ABSTRACT **Monocyte chemotactic protein 1 (MCP1) stimulates vascular smooth muscle cell (VSMC) migration in vascular wall remodeling. However, the mechanisms underlying MCP1-induced VSMC migration have not been understood. Here we identify the signaling pathway associated with MCP1-induced human aortic smooth muscle cell (HASMC) migration. MCP1, a G protein–coupled receptor agonist, activates phosphorylation of cortactin on S405 and S418 residues in a time-dependent manner, and inhibition of its phosphorylation attenuates MCP1-induced HASMC G-actin polymerization, F-actin stress fiber formation, and migration. Cortactin phosphorylation on S405/S418 is found to be critical for its interaction with WAVE2, a member of the WASP family of cytoskeletal regulatory proteins required for cell migration. In addition, the MCP1-induced cortactin phosphorylation is dependent on PLCβ3-mediated PKCδ activation, and siRNA-mediated down-regulation of either of these molecules prevents cortactin interaction with WAVE2, affecting G-actin polymerization, F-actin stress fiber formation, and HASMC migration. Upstream, MCP1 activates CCR2 and Gαq/11 in a time-dependent manner, and down-regulation of their levels attenuates MCP1-induced PLCβ3 and PKCδ activation, cortactin phosphorylation, cortactin–WAVE2 interaction, G-actin polymerization, F-actin stress fiber formation, and HASMC migration. Together these findings demonstrate that phosphorylation of cortactin on S405 and S418 residues is required for its interaction with WAVE2 in MCP1-induced cytoskeleton remodeling, facilitating HASMC migration.**

Monitoring Editor
Jonathan Chernoff
Fox Chase Cancer Center

Received: Aug 11, 2015
Revised: Oct 9, 2015
Accepted: Oct 13, 2015

INTRODUCTION

Cell migration plays an essential role in the development of organisms, repairing tissues, and defending against pathogens (Mitchison and Cramer, 1996; Stupack *et al.*, 2000). However, cell migration contributes to several pathological processes as well. To cite a few examples, migration of tumor cells, synovial fibroblasts, leukocytes, and smooth muscle cells are involved in tumor metastasis, rheumatoid arthritis, atherosclerosis, and neointimal hyperplasia, respectively (Østerud and Bjørklid, 2003; Yamaguchi *et al.*, 2005; Gerthoffer, 2007; Lefevre *et al.*, 2009). Vascular smooth muscle cell (VSMC) migration is an abnormal phenomenon underlying atherogenesis and intimal hyperplasia after angioplasty, vascular stent implantation, and organ transplantation (Clowes *et al.*, 1989; Gerthoffer, 2007). A plethora of molecules produced at the site of vascular injury by dysfunctional endothelium or inflammatory cells are involved in the modulation of VSMC migration (Berk, 2001). Monocyte chemotactic protein 1 (MCP1; also known as CCL2), in addition to its ability to attract monocytes, memory T-cells and dendritic cells in the mediation of inflammation (Carr *et al.*, 1994; Xu *et al.*, 1996), also exhibits potent chemotactic activity toward VSMCs (Singh *et al.*, 2012; Kundumani-Sridharan *et al.*, 2013). MCP1 binds to CCR2 and CCR4, which belong to the superfamily of G protein–coupled receptors (GPCRs), and transmits the cues from cell surface to inside the cell (Craig and Loberg, 2006; Deshmane *et al.*, 2009). MCP1 and its receptor CCR2 play a role in the pathogenesis of atherosclerosis (Boring *et al.*, 1998; Gu *et al.*, 1998) and intimal

This article was published online ahead of print in MBoC in Press (http://www.molbiolcell.org/cgi/doi/10.1091/mbc.E15-08-0570) on October 21, 2015.

Abbreviations used: CCR2, C-C chemokine receptor 2; CCR4, C-C chemokine receptor 4; CTTN, cortactin; GFP, green fluorescent protein; GPCR, G protein–coupled receptor; HASMC, human aortic smooth muscle cell; MCP1, monocyte chemotactic protein 1; PKC, protein kinase C; PLC, phospholipase C; shRNA, short hairpin RNA; siRNA, small interfering RNA; VSMC, vascular smooth muscle cell; WASP, Wiskott-Aldrich syndrome protein; WAVE2, Wiskott-Aldrich syndrome protein family member 2.

Address correspondence to: Gadiparthi N. Rao (rgadipar@uthsc.edu).

© 2015 Janjanam *et al.* This article is distributed by The American Society for Cell Biology under license from the author(s). Two months after publication it is available to the public under an Attribution–Noncommercial–Share Alike 3.0 Unported Creative Commons License (http://creativecommons.org/licenses/by-nc-sa/3.0).

"ASCB®," "The American Society for Cell Biology®," and "Molecular Biology of the Cell®" are registered trademarks of The American Society for Cell Biology.

hyperplasia (Roque *et al.*, 2002), although the downstream signaling events of the MCP1–CCR2 axis are not well studied.

Cell migration requires spatial and temporal coordination of cytoskeletal proteins leading to actin polymerization, and actin polymerization is mediated by a large number of actin-binding proteins (Vicente-Manzanares *et al.*, 2005). Among them, actin-related protein 2/3 (Arp2/3), cortactin, Wiskott–Aldrich syndrome proteins (WASP and N-WASP), and verprolin homologous protein 2 (WAVE2) play important roles in actin polymerization, which, in turn, facilitates cell migration (Yamaguchi and Condeelis, 2007). Arp2/3 complex is the major component of actin nucleation and mediates actin polymerization by interactions with cortactin, N-WASP, and WAVE2 (Mullins and Pollard, 1999; Suetsugu *et al.*, 2001; Uruno *et al.*, 2001). Whereas N-WASP plays a role in filopodium formation (Miki *et al.*, 1998a), WAVE2 plays a role in lamellipodium formation required for cell migration (Miki *et al.*, 1998b; Takahashi and Suzuki, 2009). Cortactin was initially identified as a Src substrate and later found to be a nucleation promoting factor (Wu *et al.*, 1991; Uruno *et al.*, 2001). The basic structure of cortactin comprises an N-terminal acidic (NTA) region, actin-binding repeats, a proline-rich region, and an SH3 domain at the C-terminal end. The NTA domain of cortactin interacts directly with Arp2/3 to activate the Arp2/3 complex and facilitates cell migration by enhancing lamellipodium formation and adhesion assembly (Weed *et al.*, 2000; Bryce *et al.*, 2005). The fourth actin-binding repeat of cortactin interacts with F-actin to facilitate lamellipodium formation (Weed *et al.*, 2000). In addition, cortactin reinforces the interaction of Arp2/3 complex with F-actin by maintaining F-actin networks from undergoing depolymerization (Weaver *et al.*, 2001). The SH3 domain present in the C-terminus binds to proteins such as N-WASP or WASP-interacting protein, which promote actin nucleation and hence actin polymerization (Kinley *et al.*, 2003; Martinez-Quiles *et al.*, 2004). The potential of cortactin to interact with several cytoskeletal and signaling proteins through its SH3 domain also links this protein to various cellular processes, including invadopodium and lamellipodium formation (Bryce *et al.*, 2005; Artym *et al.*, 2006). The capacity of cortactin to interact with many of these cytoskeletal and signaling proteins appears to be regulated by its posttranslational modifications. It was reported that phosphorylation at the Y421, Y470, or Y486 residue in the proline-rich domain is required for its role in the development of lamellipodial protrusions and cell migration (Huang *et al.*, 1998; Wang *et al.*, 2011). On the other hand, phosphorylation at S405 and S418 by Pak1 and Erks (Grassart *et al.*, 2010; Kelley *et al.*, 2010) is required for its interaction with N-WASP in activating the Arp2/3 complex, leading to actin polymerization and lamellipodium formation (Martinez-Quiles *et al.*, 2004; Kelley *et al.*, 2010). Cortactin can also be phosphorylated at S113 by Pak3 and S298/348 by protein kinase D (Webb *et al.*, 2006; Eiseler *et al.*, 2010). However, although S113 and S298 phosphorylations of cortactin have been shown to exert a negative effect on actin polymerization and cell migration, the role of S348 phosphorylation is unclear (Webb *et al.*, 2006; Eiseler *et al.*, 2010). In addition to phosphorylation, deacetylation of cortactin by HDACs is required for its interaction with F-actin and cell migration (Zhang *et al.*, 2007, 2009). In previous studies, we reported that MCP1 mediates VSMC migration and proliferation (Potula *et al.*, 2009; Singh *et al.*, 2011). We also reported that MCP1 induces HASMC F-actin stress fiber formation, migration, and proliferation via activation of NFATc1-mediated cyclin D1-CDK6-PKN1-CDK4-PAK1 signaling (Kundumani-Sridharan *et al.*, 2013; Singh *et al.*, 2012). However, the upstream signaling events of MCP1 in the modulation of HASMC migration are not known. Therefore, in the present study, we examined the role of cortactin in the mechanisms by which MCP1 induces HASMC migration. Here we show that MCP1, via activation of CCR2, Gαq/11, phospholipase Cβ3 (PLCβ3), and protein kinase Cδ (PKCδ), stimulates phosphorylation of cortactin at S405 and S418, leading to its interaction with WAVE2 and promoting actin polymerization and HASMC migration.

RESULTS

Role of cortactin phosphorylation in MCP1-induced HASMC migration

Cortactin is an actin nucleation–promoting factor and a crucial molecular scaffold for actin assembly and organization, which are necessary for endocytosis, cell migration, and invasion (MacGrath and Koleske, 2012). Serine phosphorylation of cortactin is important for cancer cell migration (Kruchten *et al.*, 2008). Therefore, to understand the mechanism of MCP1-induced HASMC migration, we tested the role of cortactin. MCP1 induces serine/threonine phosphorylation of cortactin in a time-dependent manner (Figure 1A). The S113, S298, S348, S405, and S418 residues are potential sites of phosphorylation in cortactin (MacGrath and Koleske, 2012). To determine which of these serine residues are phosphorylated, we mutated each of these serine residues to alanine by site-directed mutagenesis and tested their effects on MCP1-induced cortactin phosphorylation. Whereas S113A, S298A, and S348A mutants had no effect, the S405A and S418A mutants reduced MCP1-induced cortactin phosphorylation, suggesting that MCP1 induces phosphorylation of cortactin at S405 and S418 residues in HASMCs (Figure 1B). To determine whether cortactin mediates actin polymerization by MCP1, we immunoprecipitated cortactin from control and 2-h MCP1–treated cells and tested its effect on G-actin polymerization in vitro. The anti-cortactin immunoprecipitates of MCP1-treated cells exhibited increased G-actin polymerization compared with untreated cells (Figure 1C). In addition, overexpression of S405A and S418A mutants of cortactin prevented MCP1-induced G-actin polymerization (Figure 1D). Consistent with these observations, overexpression of S405A/S418A mutants of cortactin also attenuated HASMC F-actin stress fiber formation and migration (Figure 1, E and F), suggesting that phosphorylation of cortactin on S405 and S418 residues is required for MCP1-induced HASMC migration. To validate these findings, we also tested the effect of cortactin small interfering RNA (siRNA) on MCP1-induced HASMC F-actin stress fiber formation and migration and found that down-regulation of cortactin levels prevents HASMC F-actin stress fiber formation and migration (Figure 1, G and H).

Cortactin phosphorylation at S405 and S418 residues is required for its interaction with WAVE2

Although cortactin plays an important role in actin nucleation and polymerization, it requires interactions with other cytoskeletal proteins in mediating these effects. Toward this end, we studied its interactions with WAVE2, which also plays an important role in cell migration (Yamazaki *et al.*, 2003). Coimmunoprecipitation experiments showed that cortactin interacts with WAVE2 in a time-dependent manner (Figure 2A). To determine the role of cortactin phosphorylation in its interaction with WAVE2, we tested the effects of S405A and S418A mutants. Overexpression of S405A/S418A mutants of cortactin prevented its interaction with WAVE2 by MCP1 (Figure 2B). In addition, siRNA-mediated depletion of WAVE2 inhibited MCP1-induced G-actin polymerization, F-actin stress fiber formation, and HASMC migration (Figure 2, C–E). These observations suggest that cortactin plays an important role in MCP1-induced HASMC migration via its interaction with WAVE2, promoting G-actin polymerization and F-actin stress fiber formation.

PKCδ mediates cortactin phosphorylation in MCP1-induced HASMC migration

PKCs are key intracellular enzymes activated by calcium and diacylglycerol (DAG), alone or in combination, or independent of both of these molecules (Mellor and Parker, 1998). To determine the mechanisms underlying MCP1-induced cortactin phosphorylation, we tested the time-course effect of MCP1 on activation of conventional (α, β, γ) and novel (δ, ε, η, θ) PKCs. MCP1 induced phosphorylation of PKCδ, PKCε, and PKCθ in a time-dependent manner in HASMCs (Figure 3A). Because the time course of PKCδ and PKCε phosphorylation correlated with the time course of cortactin phosphorylation, we next focused on the role of these novel PKCs in MCP1-induced cortactin phosphorylation. Adenovirus-mediated expression of dnPKCδ blocked MCP1-induced cortactin phosphorylation and its interaction with WAVE2 (Figure 3, B and C). On the other hand, adenovirus-mediated expression of dnPKCε had no effect on MCP1-induced cortactin phosphorylation (Figure 3B). These findings suggest that PKCδ but not PKCε mediates MCP1-induced cortactin phosphorylation. Consistent with these observations, adenovirus-mediated expression of dnPKCδ also attenuated MCP1-induced G-actin polymerization, F-actin stress fiber formation, and HASMC migration (Figure 3, D–F). To confirm the role of PKCδ in MCP1-induced cortactin phosphorylation and its interaction with WAVE2, we used the siRNA approach as well. Down-regulation of PKCδ levels prevented cortactin phosphorylation and its interaction with WAVE2, which, in turn, hampered cortactin-mediated G-actin polymerization, F-actin stress fiber formation, and HASMC migration (Figure 4, A–E).

Role of PLCβ3 in PKCδ activation and cortactin phosphorylation in MCP1-induced HASMC migration

Many reports suggest that GPCR agonists activate PLCβs in mediating their cellular effects (Kelley *et al.*, 2006; Lyon *et al.*, 2014). To test the role of PLCβs in MCP1-induced cortactin phosphorylation and actin cytoskeleton remodeling, we first studied the time-course effect of MCP1 on the steady-state levels of PLCβ isoforms. MCP1 had no effect on PLCβ1-3 levels, and the presence of PLCβ4 was not detected in HASMCs (Figure 5A). Next, using a fluoregenic PLC substrate, WH-15 (Huang *et al.*, 2011), we studied the effect of MCP1 on their activities. MCP1 induced PLCβ3 but not PLCβ1 or PLCβ2 activities in a time-dependent manner in HASMCs (Figure 5B). Furthermore, depleting PLCβ3 levels by its short hairpin RNA (shRNA) expression plasmid inhibited phosphorylation of PKCδ and cortactin (Figure 5C). Furthermore, down-regulation of PLCβ3 levels using its shRNA suppressed MCP1-induced cortactin–WAVE2 interactions, G-actin polymerization, F-actin stress fiber formation, and HASMC migration (Figure 5, D–G).

CCR2 but not CCR4 activation is required for PLCβ3- and PKCδ-dependent cortactin phosphorylation in MCP1-induced HASMC migration

MCP1 mediates its effects via its receptors CCR2 and CCR4 (Craig and Loberg, 2006). However, in HASMCs, it is not known which of these receptors mediates MCP1-induced cytoskeleton remodeling, leading to their migration. Both CCR2 and CCR4 are present in HASMCs as detected by Western blot analysis, and treatment with MCP1 did not affect their steady-state levels (Figure 6A). To study the role of these receptors in MCP1-induced HASMC migration, we used their antagonists, CCR2A and CCR4A, respectively. CCR2A significantly inhibited MCP1-induced PLCβ3 activity compared with CCR4A (Figure 6B). On the other hand, MCP1-induced PKCδ phosphorylation depended on activation of either CCR2 or CCR4, although preferentially CCR2 (Figure 6C). CCR2A but not CCR4A also prevented MCP1-induced cortactin phosphorylation, cortactin–WAVE2 interactions, G-actin polymerization, F-actin stress fiber formation, and HASMC migration (Figure 6, C–G).

Gαq/11 mediates MCP1-induced PLCβ3- and PKCδ-mediated cortactin phosphorylation and HASMC migration

To understand further how CCR2 mediates the effects of MCP1 on HASMC migration, we studied the role of G proteins. Treatment with MCP1 did not affect the steady-state levels of Gαq, Gα11, Gα12, or Gα13 (Figure 7A). However, MCP1 caused a time-dependent dissociation of Gαq/11 but not Gα12 or Gα13 from CCR2 (Figure 7B), suggesting that MCP1 activates Gαq/11-coupled CCR2 receptors in HASMCs. Silencing Gαq/11 using their siRNAs prevented MCP1-induced PLCβ3 activity (Figure 7C). Down-regulation of Gαq/11 also attenuated MCP1-induced PKCδ and cortactin phosphorylation (Figure 7D). In addition, depletion of Gαq/11 levels inhibited MCP1-induced cortactin–WAVE2 interactions, G-actin polymerization, F-actin stress fiber formation, and HASMC migration (Figure 7, E–H).

DISCUSSION

Many studies have demonstrated that MCP1 is involved in vascular wall remodeling (Schober *et al.*, 2004; Singh *et al.*, 2012; Kundumani-Sridharan *et al.*, 2013). VSMC migration requires cytoskeletal remodeling (Gerthoffer, 2007). In characterizing the role of cytoskeletal remodeling in MCP1-induced VSMC migration, we found that MCP1 induces serine/threonine phosphorylation of cortactin in HASMCs. It was reported that cortactin binds to Arp2/3 and acts as a nucleation-promoting factor to enhance actin polymerization and F-actin formation, facilitating cell migration (Weed *et al.*, 2000; Uruno *et al.*, 2001; Weaver *et al.*, 2001). Previous studies showed that phosphorylation of cortactin on S405/S418 is needed for its role in actin polymerization and invadopodium and lamellipodium formation, which are required for cell migration (Ayala *et al.*, 2008; Kelley *et al.*, 2010). In the present study, we found that MCP1 induces phosphorylation of cortactin on S405 and S418 but not on S113, S298, and S348 residues, and overexpression of S405/418A mutants prevents MCP1-induced G-actin polymerization, F-actin stress fiber formation, and HASMC migration. These observations indicate that cortactin phosphorylation at S405/S418 residues is required for its role in MCP1-induced cell migration. The finding that down-regulation of cortactin levels by its siRNA inhibits G-actin polymerization, F-actin stress fiber formation, and HASMC migration also supports the role of cortactin in HASMC migration. To understand the potential mechanisms underlying the role of cortactin in the regulation of MCP1-induced HASMC migration, we found that cortactin interacts with WAVE2 and promotes actin polymerization. In addition, our results showed that phosphorylation of cortactin at S405/418 residues is essential for its interaction with WAVE2 in mediating G-actin polymerization, F-actin stress fiber formation, and HASMC migration by MCP1. Furthermore, depletion of WAVE2 levels prevented MCP1-induced G-actin polymerization, F-actin stress fiber formation, and HASMC migration. In addition, other studies showed that the C-terminal verprolin homology, cofilin homology, and acidic region domain of WAVE2 enhances the branching efficiency of actin filaments (Suetsugu *et al.*, 2001). It was also reported that cortactin in concert with N-WASP activates the Arp2/3 complex and enhances G-actin polymerization (Helgeson and Nolen, 2013). Furthermore, phosphorylation of cortactin on S405/418 is critical for its interaction with N-WASP and to activate the Arp2/3 complex (Martinez-Quiles *et al.*, 2004). On the basis of these findings, along with our observations, we suggest that the

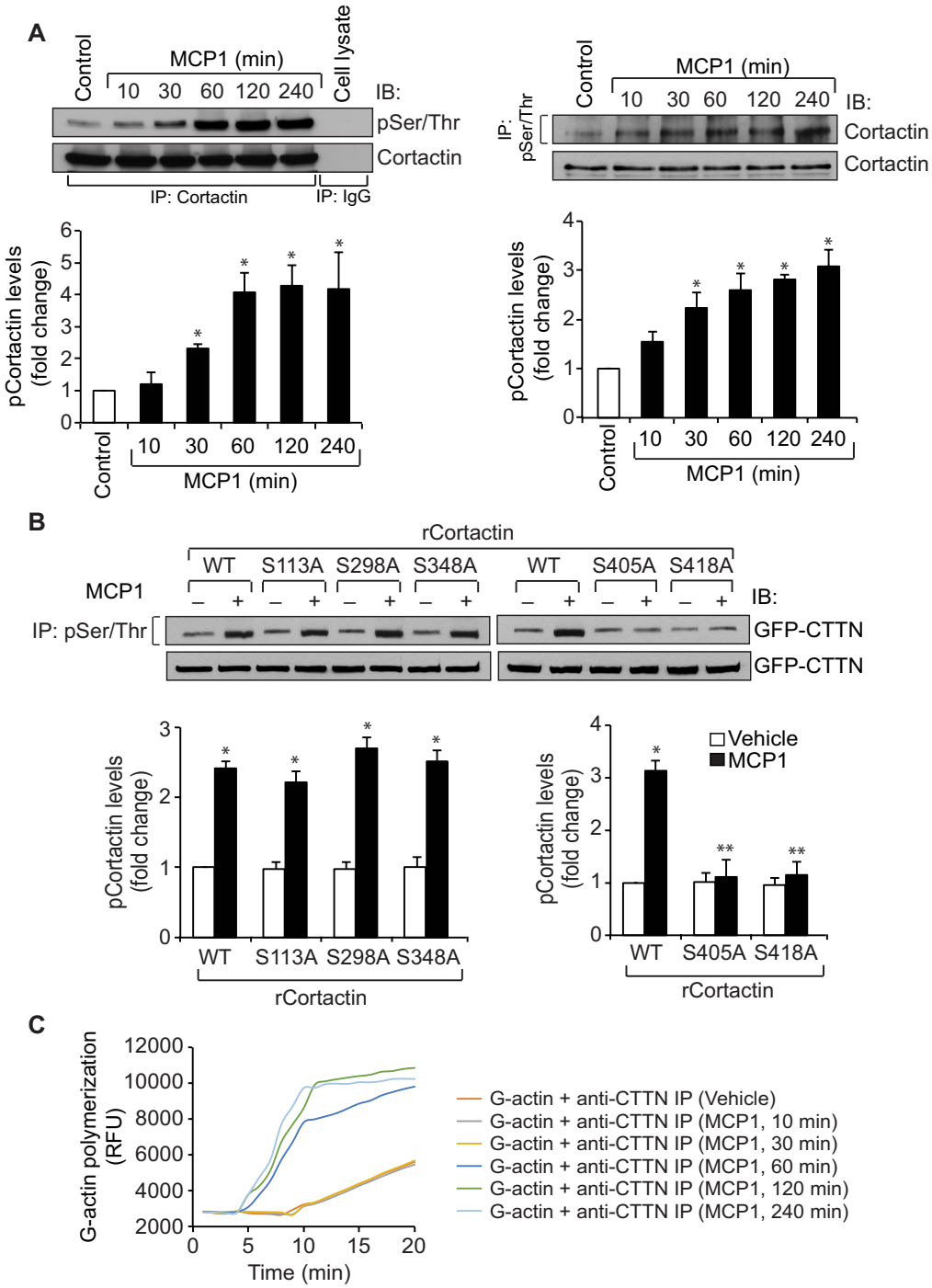

FIGURE 1: Cortactin phosphorylation at S405/S418 is required for MCP1-induced HASMC migration. (A) Quiescent HASMCs were treated with vehicle or MCP1 (50 ng/ml) for the indicated time periods, and cell extracts were prepared. Equal amounts of protein from control and each treatment were analyzed for cortactin phosphorylation by reciprocal immunoprecipitation using anti-cortactin and anti-pSer/Thr antibodies, followed immunoblotting with the indicated antibodies. Nonimmune immunoglobulin G (IgG) was used as a negative control for immunoprecipitation. (B) HASMCs were transfected with green fluorescent protein (GFP)–tagged cortactin expression vector with or without S113A, S298A, S348A, S405A, or S418A mutations, quiesced, and treated with vehicle or MCP1 for 2 h. Equal amounts of protein from control and each treatment were immunoprecipitated with anti-pSer/Thr antibodies, and the immunocomplexes were analyzed by Western blotting using anti-GFP antibodies. (C) Equal amounts of protein from control and various time periods of MCP1-treated cells were immunoprecipitated with anti-cortactin antibodies. After eluting from the immunocomplexes, cortactin was incubated with pyrene-actin monomers, and the rate of actin polymerization was measured as described in *Materials and Methods*. (D) Cells were transfected with GFP-tagged cortactin expression vector with or without S405A or S418A mutations, quiesced, and treated with vehicle or MCP1 for 2 h. Equal amounts of protein from control and each treatment were immunoprecipitated with anti-GFP antibodies. After release from the immunocomplexes, the GFP-tagged cortactin was analyzed for actin polymerization as described for C. (E) Cells were seeded onto glass coverslips in a six-well

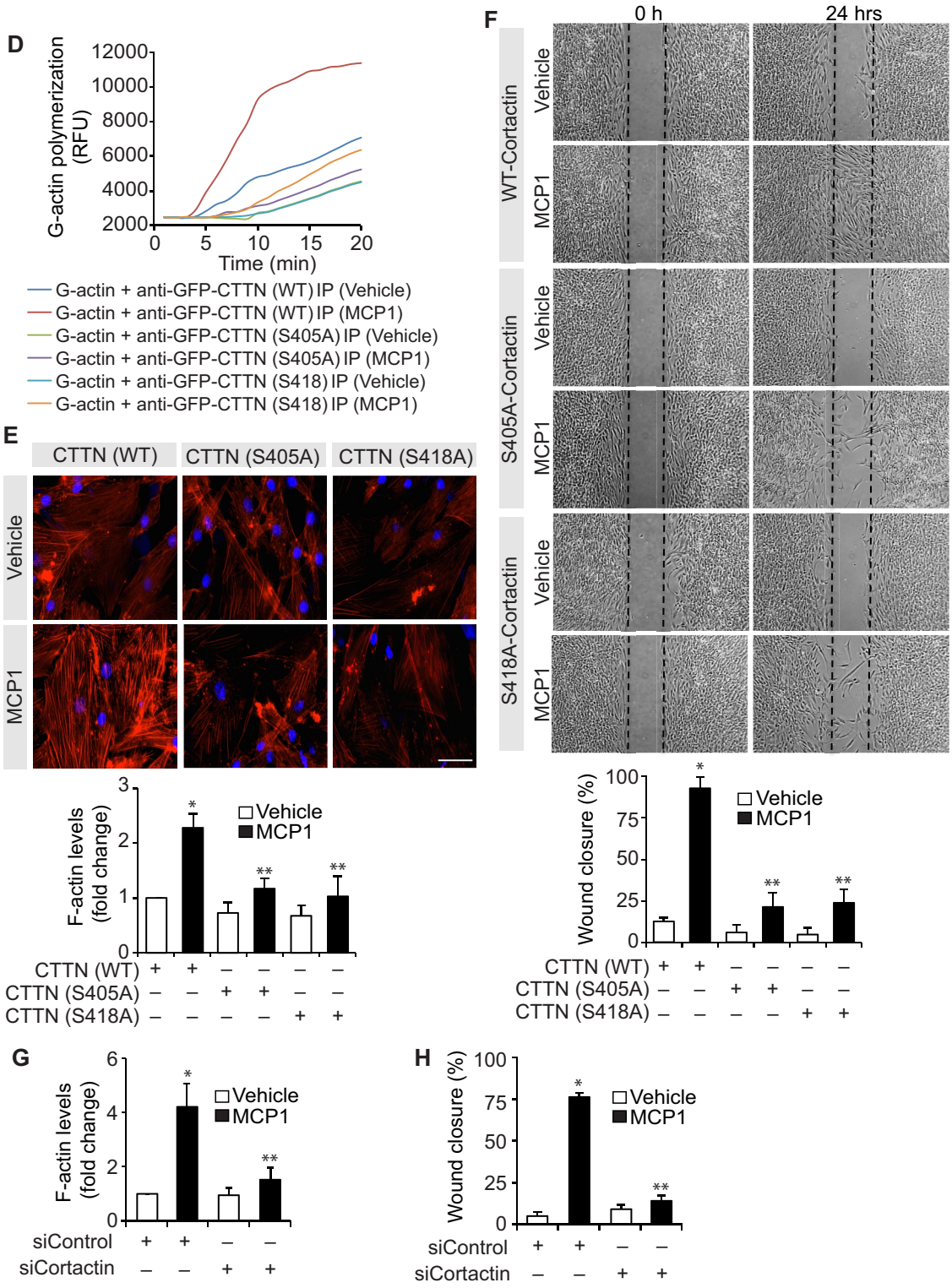

plate, transfected with GFP-tagged cortactin expression vector with or without S405A or S418A mutations, quiesced, treated with vehicle or MCP1 for 6 h, and stained for F-actin stress fiber formation with rhodamine-conjugated phalloidin. The images were captured using an inverted Zeiss fluorescence microscope (AxioObserver Z1) via a 40×/NA 0.6 objective and AxioCam MRm camera without any enhancements, and F-actin levels were quantified using ImageJ software. Scale bar, 50 µm. (F) Cells were seeded into ibidi chambers, transfected with GFP-tagged cortactin expression vector with or without S405A or S418A mutations, quiesced, and subjected to wound-healing cell migration assay in response to vehicle or MCP1 as described in *Materials and Methods*. (G) Cells were transfected with siControl or siCortactin, quiesced, treated with vehicle or MCP1 for 6 h, and stained for F-actin as described for E. (H) All the conditions were the same as for G, except that cells were subjected to wound-healing cell migration assay in response to vehicle or MCP1. The bar graphs in A, B and E–H represent mean ± SD values of three independent experiments. *$p < 0.05$ vs. vehicle control or CTTN (WT) or siControl; **$p < 0.05$ vs. MCP1, CTTN (WT) + MCP1, or siControl + MCP1.

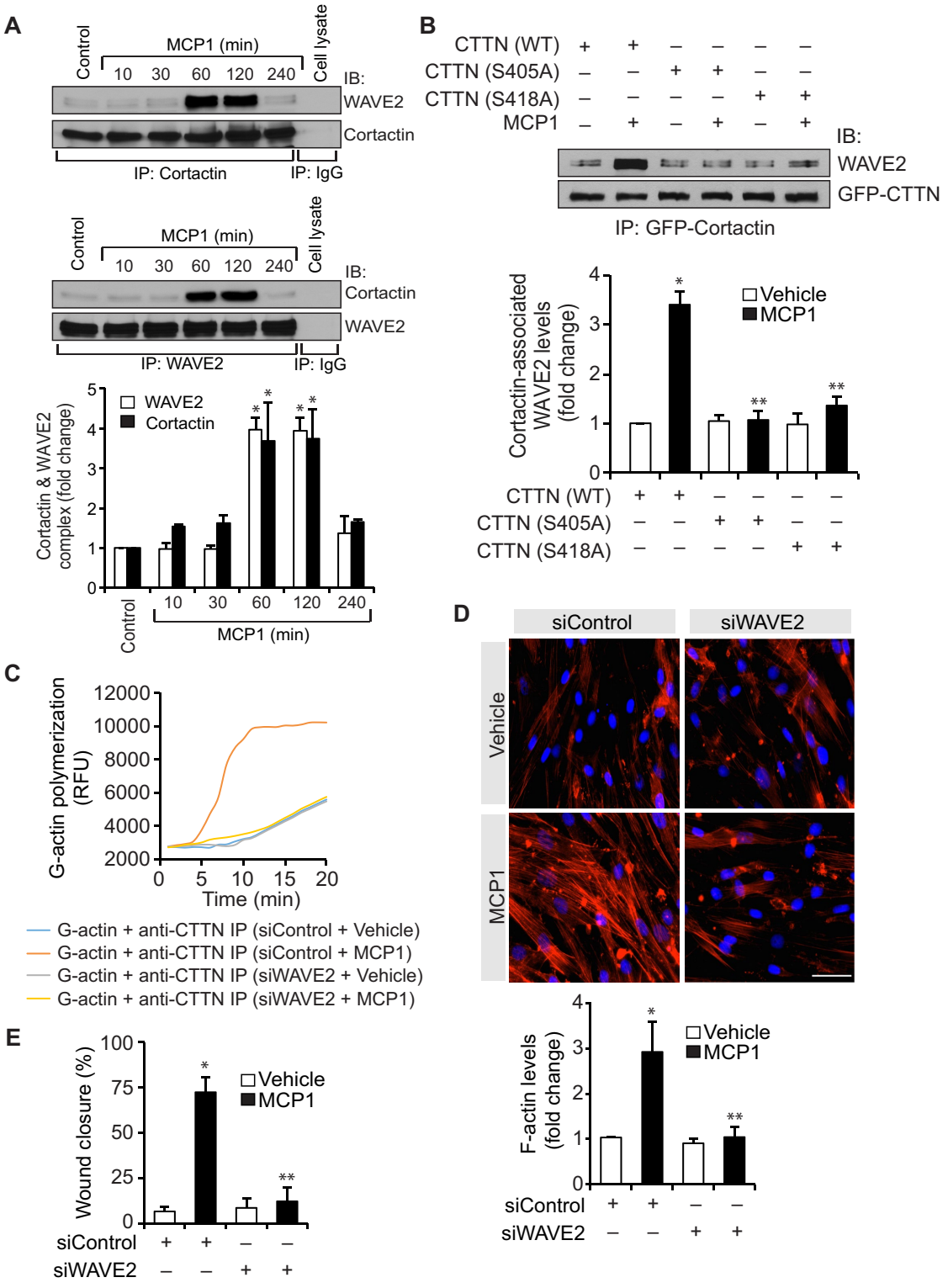

FIGURE 2: Cortactin phosphorylation at S405/S418 is essential for its interaction with WAVE2 in HASMC migration. (A) Quiescent cells were treated with vehicle or MCP1 for the indicated time periods, and cell extracts were prepared. Equal amounts of protein from control and each treatment were immunoprecipitated with anti-cortactin or anti-WAVE2 antibodies, and the immunocomplexes were analyzed by immunoblotting with the indicated antibodies. Nonimmune IgG was used as a negative control for immunoprecipitation. (B) HASMCs were transfected with GFP-tagged cortactin expression vector with or without S405A or S418A mutations, quiesced, and treated with vehicle or MCP1 for 2 h. Equal amounts of protein from control and each treatment were immunoprecipitated with anti-GFP antibodies, followed by immunoblotting with the indicated antibodies. (C) Cells were transfected with siControl or siWAVE2, quiesced, and treated with vehicle or MCP1 for 2 h, and equal amounts of protein from control and each treatment were immunoprecipitated with anti-cortactin antibodies. After elution from the immunocomplexes, the cortactin was

cortactin–WAVE2 interactions probably intensify the actin branching that is required for MCP1-induced HASMC migration.

In elucidating the upstream mechanisms of cortactin phosphorylation by MCP1, we observed that MCP1 activates PKCδ and PKCε with a time course that overlaps the time course of cortactin phosphorylation. However, adenovirus-mediated expression of dnPKCδ but not dnPKCε inhibited MCP1-induced cortactin phosphorylation at S405/418. Down-regulation of PKCδ levels by its siRNA also inhibited MCP1-induced cortactin phosphorylation. These results indicate that PKCδ but not PKCε mediates MCP1-induced cortactin phosphorylation. Previous reports showed that Pak1, Mek, or Erks can phosphorylate cortactin on S405 and S418 residues (Martinez-Quiles *et al.*, 2004; Grassart *et al.*, 2010; Kelley *et al.*, 2010). It was also reported that PKCδ interacts with cortactin and organizes actin dynamics in early endosomes (Llado *et al.*, 2008). Other reports have shown that cortactin is phosphorylated at S113 by Pak3 and at S298/348 by protein kinase D (Webb *et al.*, 2006; Eiseler *et al.*, 2010). However, in our study, MCP1 does not stimulate cortactin phosphorylation at S113, S298, or S348. In addition, our findings reveal that MCP1-induced activation of PKCδ is critical for actin polymerization, F-actin stress fiber formation, and HASMC migration. Other reports have shown that PKCδ by myosin light chain phosphorylation mediates epidermal growth factor–induced fibroblast contractility and motility (Iwabu *et al.*, 2004). PKCδ also promotes smooth muscle cell migration by platelet-derived growth factor-BB (PDGF-BB) or mechanical stress (Li *et al.*, 2003; Kamiya *et al.*, 2007). Another study demonstrated that lysophosphatidic acid induces fibroblast migration via phosphorylation and activation of PKCδ (Gan *et al.*, 2012). In view of all of these findings, we suggest that PKCδ via phosphorylation of cytoskeletal or contractile proteins mediates the migration of various cell types in response to different agonists.

PLCs are widely expressed enzymes that hydrolyze phosphatidylinositol 4,5-bisphosphate and generate inositol 1,4,5-trisphosphate and DAG (Berridge and Irvine, 1989). Because novel PKCs require DAG for their activation, we examined the role of PLCβs in MCP1-induced PKCδ activation. We observed that MCP1 stimulates PLCβ3 activity with a time course that overlaps the time course of PKCδ phosphorylation. We further discovered that PLCβ3, via PKCδ, mediates MCP1-induced cortactin phosphorylation, cortactin/WAVE2 interactions, G-actin polymerization, F-actin stress fiber formation, and HASMC migration. Previous studies showed that activation of PLCβ2/3 is essential for chemoattractant-mediated regulation of PKCs, and loss of both genes prevented PKC activation and T-cell migration (Li *et al.*, 2000; Bach *et al.*, 2007). On the basis of these observations and present findings, we suggest that various PLCβs, by activating different PKCs, play an important role in the modulation of cell migration.

Many studies suggest that Gα or Gβγ subunits of Gq/11 heterotrimeric G proteins regulate PLCβs (Smrcka and Sternweis, 1993; Biber *et al.*, 1997). We investigated the role of MCP1 receptors and G proteins in the regulation of PLCβ3 activity. We found that CCR2 but not CCR4 mediates PLCβ3 activity. Although CCR2 couples to various G proteins, including Gq/11, G14/16 and Gi (Arai and Charo, 1996; Kuang *et al.*, 1996), in response to MCP1, only Gαq/11 dissociates from CCR2, indicating that MCP1 activates Gq/11 downstream of CCR2. Furthermore, like CCR2, down-regulation of Gαq/11 completely inhibited MCP1-induced PLCβ3 and PKCδ activation and cortactin phosphorylation, resulting in diminished F-actin stress fiber formation and HASMC migration. Our findings are also consistent with previous reports that Gαq/11 directly activates PLCβ3 (Lyon *et al.*, 2013). A role for Gαq/11 in endothelial and neuronal cell migration has also been demonstrated (Zeng *et al.*, 2002; Ando *et al.*, 2010).

It is important to note that despite the presence of both the receptors, only CCR2 and not CCR4 mediates MCP1-induced cortactin phosphorylation and its interaction with WAVE2 in facilitating G-actin polymerization, F-actin stress fiber formation, and HASMC migration via activation of Gαq/11-PLCβ3-PKCδ signaling. However, CCR4 was partially involved in PKCδ activation by MCP1. Because CCR4 had no major role in HAMSC migration, this observation may indicate that the CCR4-dependent PKCδ activation might be linked to other responses of HASMCs to MCP1. It was demonstrated that CCR2 mediates MCP1-induced VSMC migration and proliferation in neointimal development (Roque *et al.*, 2002). In addition, other reports showed that CCR2 mediates MCP1-induced human adventitial and eosinophilic leukemia cell migration (Lee *et al.*, 2009; Si *et al.*, 2012). MCP1 and CCR2 have also been shown to enhance macrophage accumulation and immune responses in the pathogenesis of atherosclerosis (Boring *et al.*, 1998; Charo, 1999; Gu *et al.*, 1999). On the basis of all of these observations and as shown in Figure 8, we speculate that CCR2, upon activation by MCP1, triggers Gαq/11-PLCβ3-PKCδ–dependent cortactin phosphorylation and its interaction with WAVE2 in the modulation of HASMC migration and thereby restenosis.

MATERIALS AND METHODS

Reagents

Anti-CCR4 antibody (AF5207), donkey anti-sheep horseradish peroxidase (HRP) antibody (HAF016), and recombinant human MCP1 (279-MC/CF) were from R&D Systems (Minneapolis, MN). CCR2 antagonist (SC-202525), CCR4 antagonist (SC-221406), and anti-cortactin (SC-11408), anti-Gαq (SC-393), anti-Gα11 (SC-394; SC-390382), anti-Gα12 (SC-409), anti-Gα13 (SC-410), anti-GFP (SC-9996), bovine anti-goat HRP (SC-2350), anti-PKCα (SC-208), anti-PKCγ (SC-211), anti-PKCδ (SC-937), anti-PKCθ (SC-212), anti-PKCε (SC-1681), and anti–β-tubulin (SC-9104) antibodies were from Santa Cruz Biotechnology (Santa Cruz, CA). Anti-cortactin (3502), anti-pPKCα/β (9375), anti-pPKCγ (9379), anti-pPKCδ (9374), anti-pPKCθ (9377), and anti-WAVE2 (3659) antibodies were purchased from Cell Signaling Technology (Beverly, MA). Anti–phosphoserine/threonine antibody (ab17464) was bought from Abcam (Cambridge, MA). Goat anti-rabbit HRP (31460) and goat anti-mouse HRP (31437) antibodies were obtained from Thermo Scientific (Waltham, MA). Protein A Sepharose CL-4B (170780-01), Protein G Sepharose Fast flow (17061801), and ECL Western blotting detection reagents (RPN2106) were from GE Healthcare (Pittsburgh, PA). Human cortactin siRNA (ON-TARGETplus SMARTpool L-010508-00-0005), human Gαq siRNA (ON-TARGETplus SMARTpool J-008562), human Gα11

incubated with pyrene-actin monomers, and the rate of actin polymerization was measured as described in *Materials and Methods*. (D) All of the conditions were same as for C, except that after quiescence, the cells were treated with vehicle or MCP1 for 6 h and stained for F-actin. (E) All of the conditions were the same as for C, except that cells were subjected to wound-healing migration assay in response to vehicle or MCP1. The bar graphs in A, B, D, and E represent mean ± SD values of three independent experiments. *$p < 0.05$ vs. vehicle control or CTTN (WT) or siControl; **$p < 0.05$ vs. MCP1, CTTN (WT) + MCP1, or siControl + MCP1.

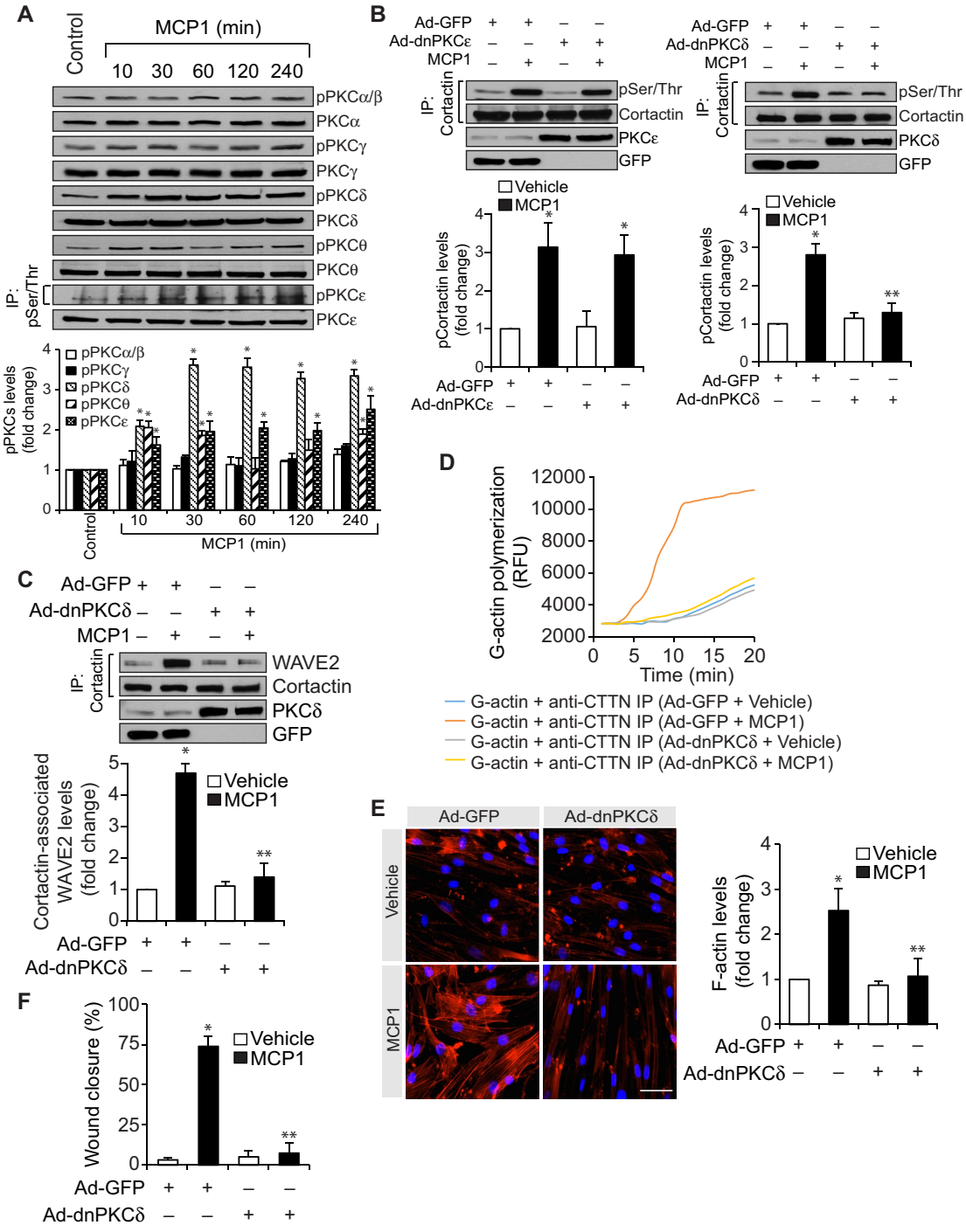

FIGURE 3: PKCδ mediates MCP1-induced cortactin phosphorylation and its interaction with WAVE2 in HASMC migration. (A) Extracts of control and the indicated time periods of MCP1-treated HASMCs were analyzed for phosphorylation of the indicated PKC isoform either by Western blotting using their phosphospecific antibodies or immunoprecipitation with anti-pSer/Thr antibody followed by immunoblotting with the indicated anti-PKC isoform antibody. (B, C) HASMCs that were infected with ad-GFP, ad-dnPKCδ, or ad-dnPKCε and quiesced were treated with vehicle or MCP1 for 2 h, and cell extracts were prepared. Equal amounts of protein from control and each treatment were immunoprecipitated with anti-cortactin antibody, and the immunocomplexes were analyzed by Western blotting for the indicated proteins. Equal amounts of protein from the same cell extracts were also analyzed by Western blotting for GFP, PKCδ, and PKCε levels to show the overexpression of GFP, dnPKCδ, and dnPKCε. (D) All of the conditions were the same as for B, except that equal amounts of protein from control and each treatment were immunoprecipitated with anti-cortactin antibody, and eluted cortactin was assayed for actin polymerization as described in Figure 1C. (E) All of the conditions were the same as for B, except that after quiescence, the cells were treated with vehicle or MCP1 for 6 h and stained for F-actin. (F) All of the conditions were the same as for B, except that after quiescence, the cells were subjected to wound-healing migration assay in response to vehicle or MCP1. The bar graphs in A–C, E, and F represent mean ± SD values of three experiments. *$p < 0.05$ vs. vehicle control or ad-GFP; **$p < 0.05$ vs. control + MCP1 or ad-GFP + MCP1.

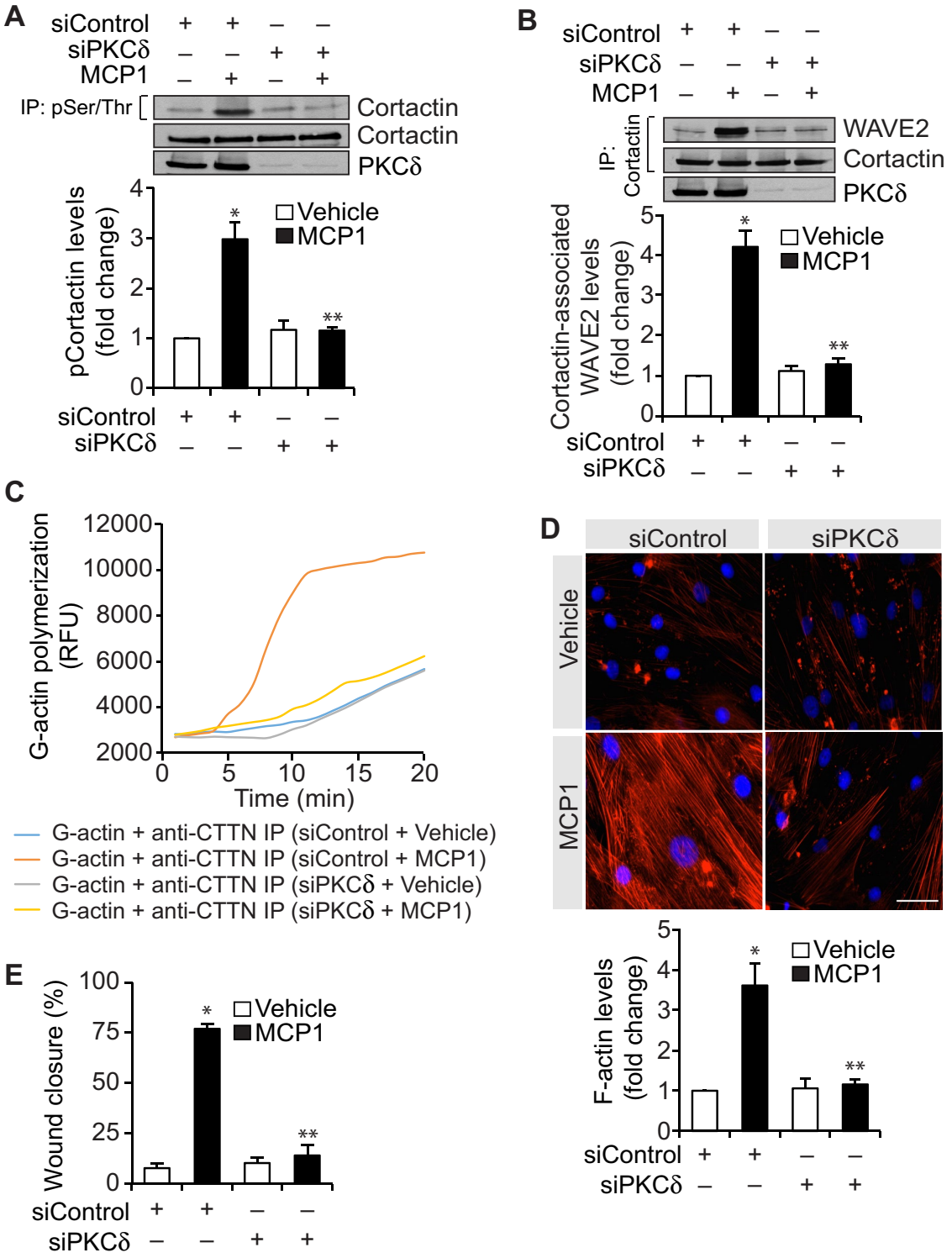

FIGURE 4: Depletion of PKCδ levels inhibited MCP1-induced cortactin phosphorylation and its interaction with WAVE2 in HASMC migration. (A, B) HASMCs that were transfected with control or PKCδ siRNA and quiesced were treated with vehicle or MCP1 for 2 h, and cell extracts were prepared. Equal amounts of protein from control and each treatment were immunoprecipitated with anti-pSer/Thr or anti-cortactin antibodies, and the immunocomplexes were analyzed by Western blotting for the indicated proteins. Equal amounts of protein from the same cell extracts from each condition were also analyzed by Western blotting for PKCδ levels to show the efficacy of the siRNA on its target molecule level. (C) An equal amount of protein from cell extracts prepared as for A was immunoprecipitated with anti-cortactin antibodies, and the cortactin was eluted from the immunocomplexes and assayed for actin polymerization as described in Figure 1C. (D) All of the conditions were the same as for A, except that after quiescence, the cells were treated with vehicle or MCP1 for 6 h and stained for F-actin. (E) All of the conditions were the same as for A, except that after quiescence, the cells were subjected to wound-healing migration assay in response to vehicle or MCP1. The bar graphs in A, B, D, and E represent mean ± SD values of three experiments. *$p < 0.05$ vs. vehicle control or siControl; **$p < 0.05$ vs. siControl + MCP1.

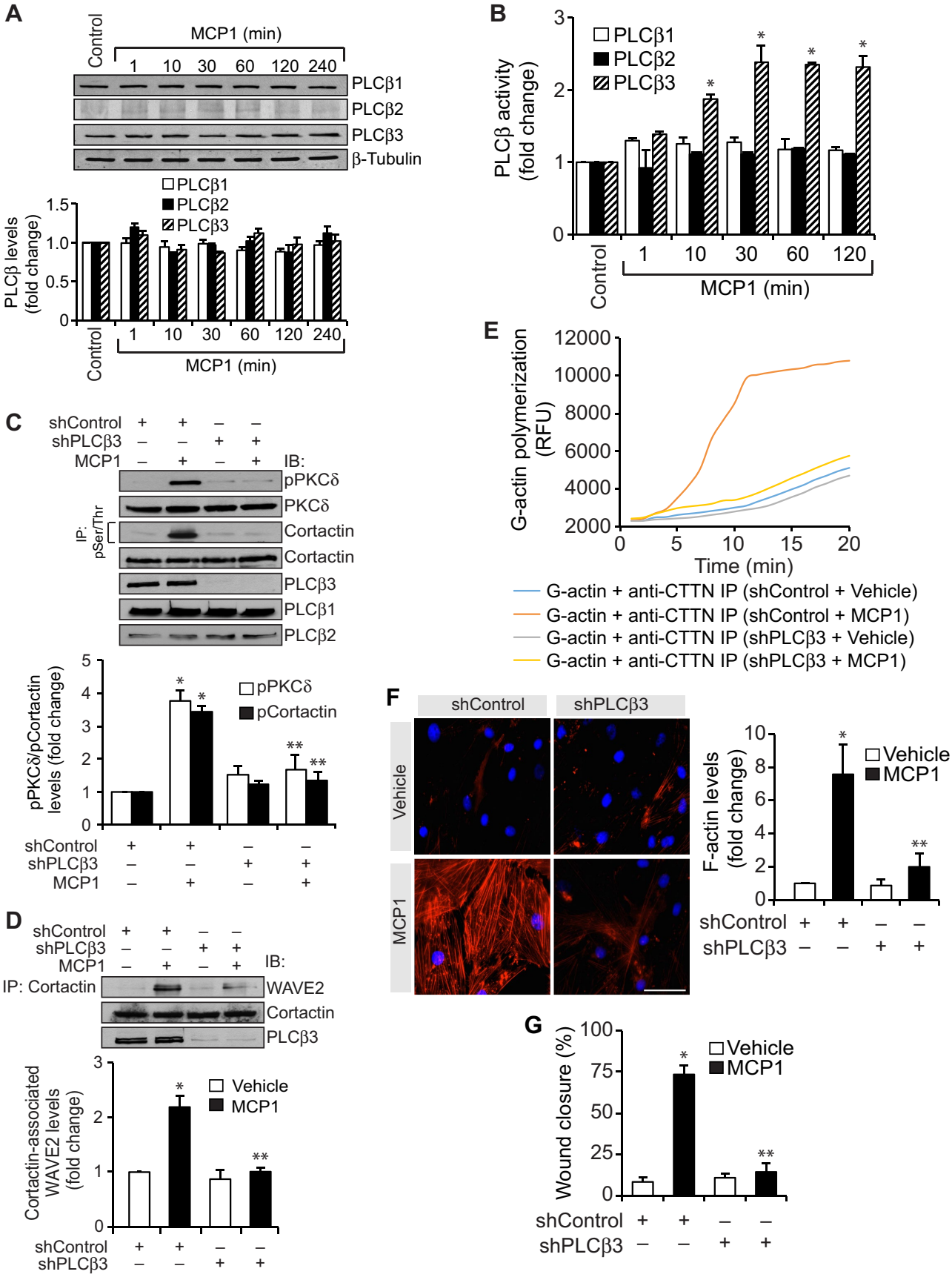

FIGURE 5: PLCβ3 acts upstream of PKCδ in MCP1-induced cortactin phosphorylation and its interaction with WAVE2 in HASMC migration. (A) Cell extracts of control and the indicated time periods of MCP1-treated HASMCs were analyzed for PLCβ1-3 levels by Western blotting using their specific antibodies and normalized for β-tubulin levels. (B) The same

siRNA (ON-TARGETplus SMARTpool J-010860), human PKCδ siRNA (ON-TARGETplus SMARTpool L-003524-00-0005), human WAVE2 siRNA (ON-TARGETplus SMARTpool L-012141-00-0010), and control nontargeting siRNA (D-001810-10) were purchased from Dharmacon RNAi Technologies (Chicago, IL). Lipofectamin 3000 transfection reagent (L3000-015), Hoechst 33342 (H3570), Prolong gold antifade mounting medium (P36930), Medium 231 (M231-500), smooth muscle growth supplements (S-007-25), and gentamicin/amphotericin solution (R-015-10) were purchased from Life Technologies (Carlsbad, CA), anti-CCR2 antibody (NB110-55674) from Novus Biologicals (Littleton, CO), and rhodamine-phalloidin (00027) from Biotium (Hayward, CA).

Cell culture

HASMCs were purchased from Invitrogen (Carlsbad, CA) and subcultured in Medium 231 containing smooth muscle cell growth supplements and 1× gentamicin/amphotericin. The cells were used between four and 10 passages for all of the experiments.

Adenoviral vectors and DNA constructs

Construction of Ad-GFP, Ax-PKC D/Nδ (Ad-dnPKCδ), and Ax-PKC D/Nε (Ad-dnPKCε) was described previously (Matsumura *et al.*, 2003; Bajpai *et al.*, 2007). pGFP cortactin was a gift from Kenneth Yamada (National Institute of Dental and Cranial Research, National Institutes of Health, Bethesda, MD; Addgene plasmid #50728). The serine (S) residues at 113, 298, 348, 405, and 418 of cortactin were mutated to alanine (A) in pGFP-cortactin mammalian expression vector using a QuikChange Lightening Site-Directed Mutagenesis Kit (Agilent Technologies) and the following primers. S113A mutant: forward, 5′-TTTCCAAGCACTGC**G**CGCAGGTGGACTCG-3′; reverse, 5′-CGAGTCCACCTGCG**C**GCAGTGCTTGGAAA-3′. S298A mutant: forward, 5′-TGGCCAAGCACGAG**G**CCCAGCAAGACTAC-3′; reverse, 5′-GTAGTCTTGCTGGG**C**CTCGTGCTTGGCCA-3′. S348A mutant: forward, 5′-GAAGCTGTGACCAGCAAAACA**GC**TAACATCAGAGCTAACTTTGA-3′; reverse, 5′-TCAAAGTTAGCTCTGATGTTA**GC**TGTTTTGCTGGTCACAGCTTC-3′. S405A mutant: forward, 5′-CGCCCCCTGTG**G**CGCCCGCACCT-3′; reverse, 5′-AGGTGCGGGCG**C**CACAGGGGGCG-3′. S418A mutant: forward, 5′-GAGGCTGCCCTCG**GC**CCCCGTCTATGAG-3′; reverse, 5′-CTCATAGACGGGG**GC**CGAGGGCAGCCTC-3′. The mutant nucleotides are shown as bold letters. DNA sequencing using vector-specific primers verified the mutations. PLCβ3 shRNA expression plasmid was constructed using BLOCK-iT U6 RNAi Entry Vector (Life Technologies) following the manufacturer's instructions. Briefly, single-stranded DNA oligos encoding PLCβ3 shRNA (top strand, 5′-**CACCG**CGGGAGTAAGTTCATCAAATCGAAATTTGATGAACTTACTCCCGC-3′; bottom strand, 5′-**AAAA**GCGGGAGTAAGTTCATCAAATTTCGATTTGATGAACTTACTCCCG**C**-3′) and scrambled shRNA (top strand, 5′-**CACCG**AATTCTCCGAACGTGTCACGTTCAAGAGACGTGACACGTTCGGAGAATT-3′; bottom strand, 5′-**AAAA**AATTCTCCGAACGTGTCACGTCTCTTGAACGTGACACGTTCGGAGAATT**C**-3′) were annealed and cloned into pENTR/U6 linear vector with overhangs. The complementary nucleotide overhangs in the primer sequences necessary for directional cloning are shown in bold letters. The positive constructs were confirmed by DNA sequencing. The EndoFree Plasmid Maxi Kit (Qiagen, Valencia, CA) was used to purify plasmids for all transfection purposes.

Transfections

HASMCs were transfected with nontargeted control or ON-TARGETplus SMARTpool siRNA at a final concentration of 100 nM using Lipofectamine 3000 transfection reagent according to the manufacturer's instructions. Wherever appropriate, cells were transfected with plasmid DNAs at a final concentration of 2.5 μg/60-mm culture dish or 5 μg/100-mm culture dish using Lipofectamine 3000 transfection reagent according to the manufacturer's instructions. After transfections, cells were recovered in complete medium overnight, growth arrested for 36 h in serum-free medium, and used as required.

Cell migration

Cell migration was measured by wound-healing assay using culture inserts (ibidi USA, Madison, WI) as described previously (Singh *et al.*, 2015) with minor modifications. Briefly, HASMCs were seeded onto the culture inserts, allowed to grow for 24–48 h and quiesced. Transfections, wherever appropriate, were performed 1 d after seeding and quiesced for 24 h. Cell growth was arrested by the addition of 5 mM hydroxyurea at the start of the experiment. Images were captured at the indicated time points using an inverted microscope (Eclipse TS100; Nikon, Melville, NY) with 4×/numerical aperture (NA) 0.13 objective. Wound closure was measured by subtracting wound area at 24 h from that at 0 h by using ImageJ software (National Institutes of Health, Bethesda, MD). Cell migration was presented as percentage of wound closure.

Immunofluorescence staining

Immunofluorescence staining for F-actin was performed as described previously (Kundumani-Sridharan *et al.*, 2013) with slight modifications. Briefly, HASMCs were seeded onto glass coverslips, allowed to grow for 24–48 h, and quiesced. After appropriate treatments, cells were fixed with 3.7% paraformaldehyde in phosphate-buffered saline (PBS) for 15 min, permeabilized in 0.3% Triton X-100 for 15 min, and blocked with 3% bovine serum albumin (BSA) in PBS. Cells were stained with rhodamine-labeled phalloidin for 1 h at room temperature. After washing with PBS, cells were counterstained with Hoechst 33342 for 5 min at room temperature and mounted onto glass slides with Prolong Gold antifade mounting medium. Fluorescence images

cell extracts prepared as for A were also analyzed for PLCβ1-3 activities as described in *Materials and Methods*.
(C, D) HASMCs that were transfected with control or PLCβ3 shRNA plasmids and quiesced were treated with vehicle or MCP1 for 2 h, and cell extracts were prepared. Equal amounts of protein from control and each treatment were immunoprecipitated with anti-pSer/Thr or anti-cortactin antibodies, and the immunocomplexes were analyzed by Western blotting for the indicated proteins. Equal amounts of protein from the same cell extracts from each condition were also analyzed by Western blotting for PLCβ1-3 levels to show the efficacy of the shRNA on its target and off-target molecule levels. (E) Equal amounts of protein from cell extracts prepared as for C were immunoprecipitated with anti-cortactin antibodies, and the cortactin was eluted from the immunocomplexes and assayed for actin polymerization as described in Figure 1C. (F) All of the conditions were the same as for C, except that after quiescence, the cells were treated with vehicle or MCP1 for 6 h and stained for F-actin. (G) All of the conditions were the same as for C, except that after quiescence, the cells were subjected to wound-healing migration assay in response to vehicle or MCP1. The bar graphs in B, D, F, and G represent mean ± SD values of three experiments. *$p < 0.05$ vs. vehicle control or control shRNA; **$p < 0.05$ vs. control shRNA + MCP1.

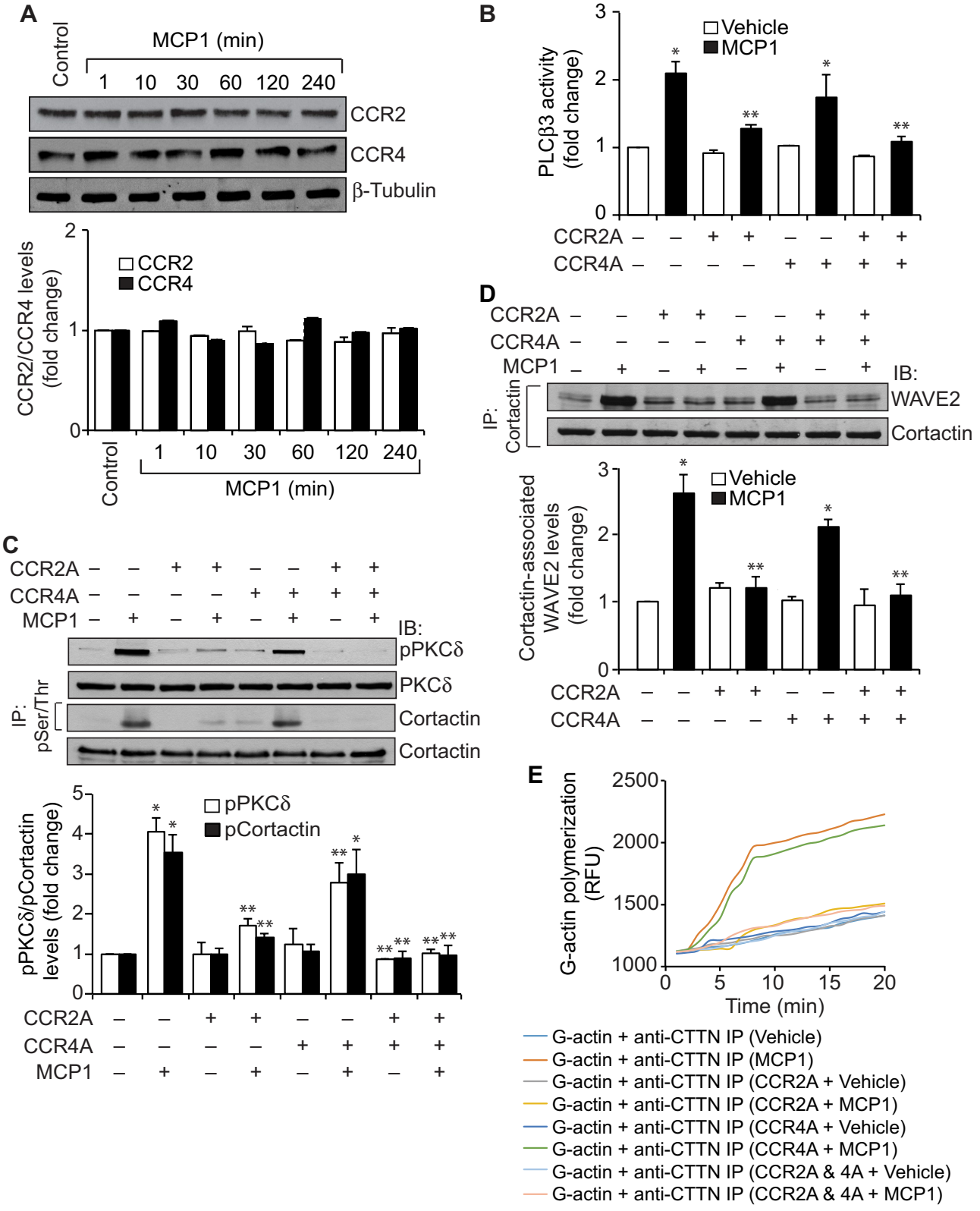

FIGURE 6: CCR2 mediates cortactin phosphorylation and its interaction with WAVE2 in HASMC migration. (A) Quiescent HASMCs were treated with vehicle or MCP1 for the indicated time periods, and cell extracts were prepared. Equal amounts of protein from control and each treatment were analyzed by Western blotting for CCR2 and CCR4 levels using their specific antibodies and normalized to β-tubulin. (B–D) Quiescent cells were treated with vehicle or MCP1 in the presence and absence of CCR2 antagonist (CCR2A) or CCR4 antagonist (CCR4A) for 30 min, and cell extracts were prepared. Equal amounts of protein from control and each treatment were analyzed for PLCβ3 activity, pPKCδ and pCortactin levels, and cortactin–WAVE2 interactions as described for Figures 5B, 3A, 1A, and 2A,

of cells were captured via an inverted Zeiss fluorescence microscope (AxioObserver Z1) with 40×/NA 0.6 objective and AxioCam MRm camera without any enhancements using the microscope operating and image analysis software AxioVision, version 4.7.2 (Carl Zeiss Imaging Solutions, Jena, Germany). The intensity of F-actin staining was measured using ImageJ software.

Immunoprecipitation

Cells with and without the indicated treatments were rinsed with cold PBS and lysed in 400 µl of lysis buffer (1% Nonidet P40, 0.5% sodium deoxycholate, 0.1% SDS, 100 µg/ml phenylmethylsulfonyl fluoride, 100 µg/ml aprotinin, 1 µg/ml leupeptin, and 1 mm sodium orthovanadate in PBS) for 20 min on ice. The cell extracts were cleared by centrifugation at 14,000 rpm for 20 min at 4°C. The cleared cell extracts containing an equal amount of protein from control and each treatment were incubated with appropriate antibody overnight at 4°C, followed by incubation with protein A/G–Sepharose CL4B beads for 3 h with gentle rocking. The beads were collected by centrifugation at 1000 rpm for 2 min at 4°C and washed four times with lysis buffer and once with PBS.

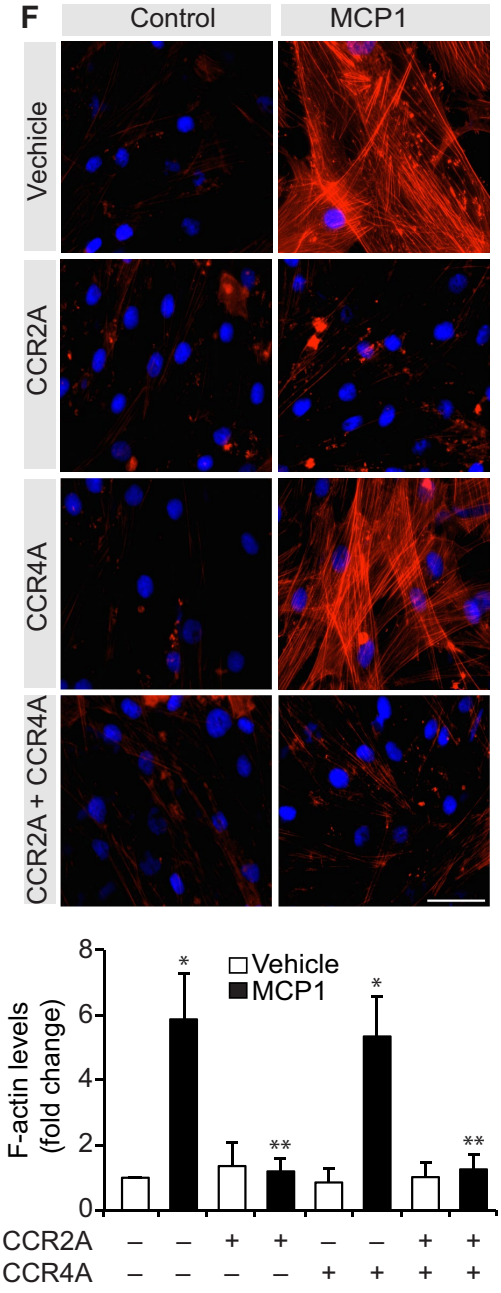

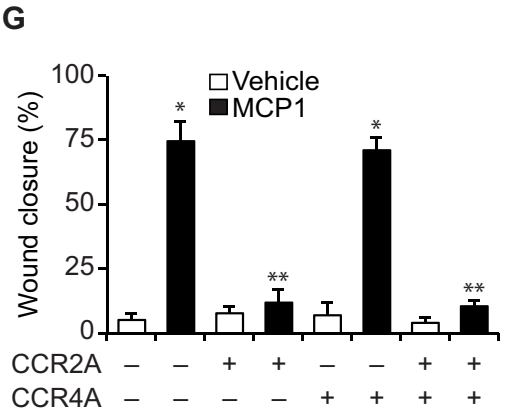

respectively. (E) Cell extracts prepared as for B were analyzed for actin polymerization as describe in Figure 2C. (F) All of the conditions were the same as for B, except that after quiescence, the cells were treated with vehicle or MCP1 for 6 h and stained for F-actin. (G) All of the conditions were the same as for B, except that after quiescence, the cells were subjected to wound-healing migration assay in response to vehicle or MCP1. The bar graphs in A–D, F, and G represent mean ± SD values of three experiments. *$p < 0.05$ vs. vehicle control; **$p < 0.05$ vs. MCP1.

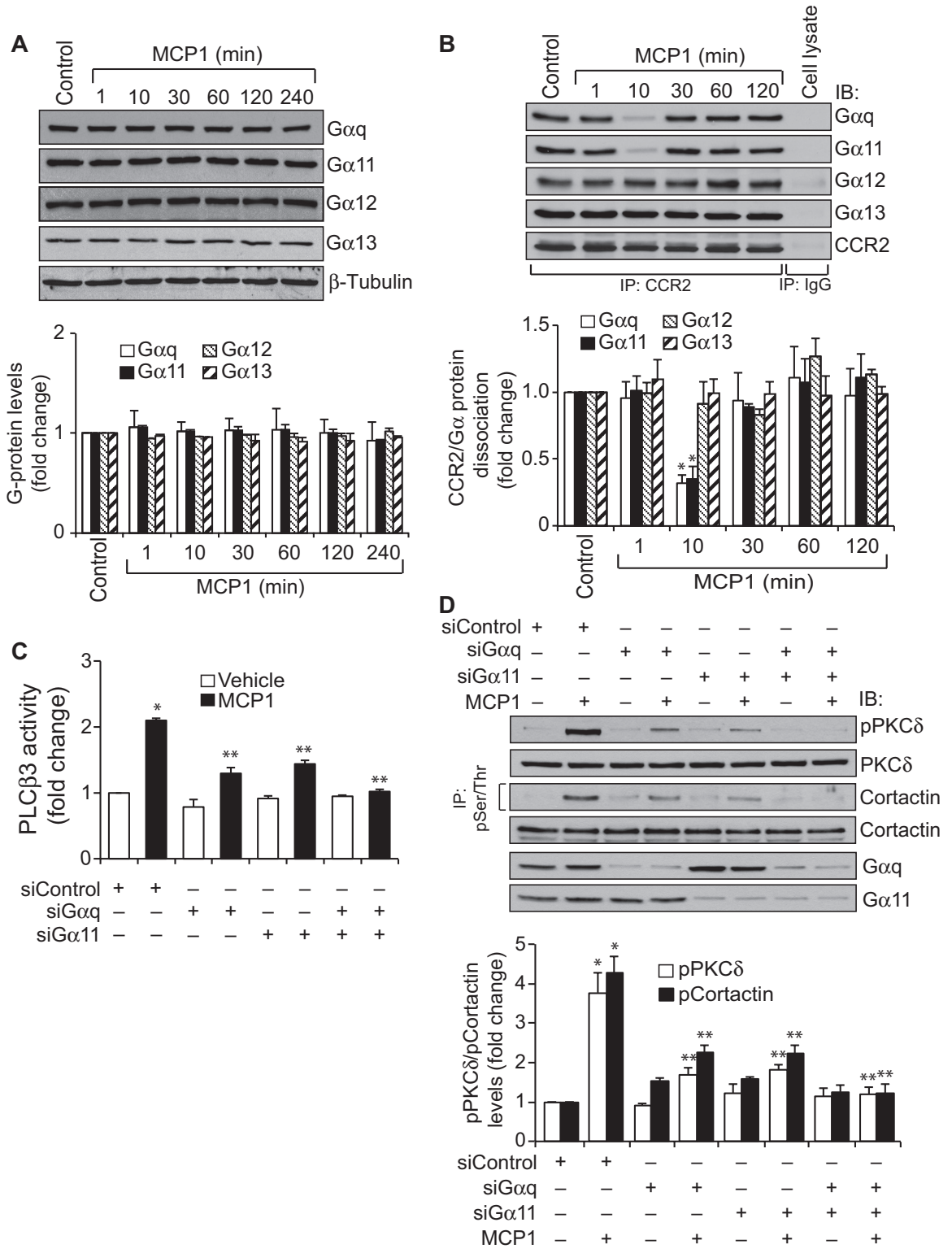

FIGURE 7: Gαq/11 mediates cortactin phosphorylation and its interaction with WAVE2 in HASMC migration. (A) Quiescent cells treated with vehicle or MCP1 for the indicated time periods, and cell extracts were prepared. Equal amounts of protein from control and each treatment were analyzed by Western blotting for Gαq, Gα11, Gα12, and Gα13 levels using their specific antibodies and normalized to β-tubulin levels. (B) All of the conditions were the same as for A, except that equal amounts of protein from control and each treatment were immunoprecipitated with anti-CCR2 antibodies, and the immunocomplexes were analyzed by Western blotting for the indicated proteins. Nonimmune IgG was used as a negative control for immunoprecipitation. (C–E) HASMCs that were transfected with siControl, siGαq, or siGα11 and quiesced were treated with vehicle or MCP1 for 30 min, and cell extracts were prepared. Equal amounts of protein from control and each treatment were analyzed for PLCβ3 activity, pPKCδ and

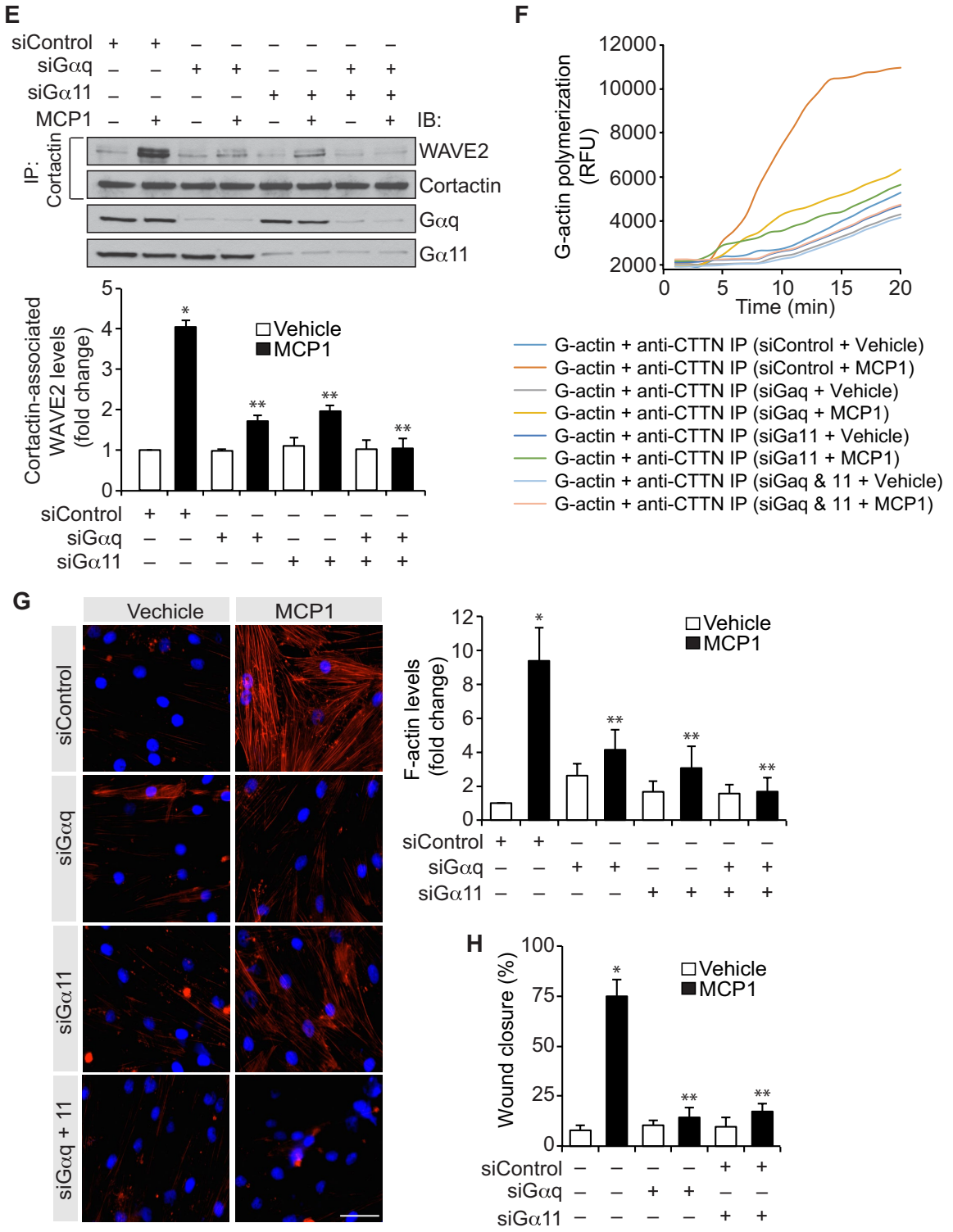

pCortactin levels, and cortactin-WAVE2 interactions as described in Figures 5B, 3A, 1A, and 2A, respectively. Equal amounts of protein from the same cell extracts were also analyzed by Western blotting for Gαq and Gα11 levels to show the efficacy of the siRNA on its target molecule level. (F) Equal amounts of protein from cell extracts prepared as for C were analyzed for actin polymerization as described in Figure 1C. (G) All of the conditions were same as for C, except that after quiescence, the cells were treated with vehicle or MCP1 for 6 h and stained for F-actin. (H) All of the conditions were same as for C, except that after quiescence, the cells were subjected to wound-healing migration assay in response to vehicle or MCP1. The bar graphs in A–E and G–H represent mean ± SD values of three experiments. *$p < 0.05$ vs. vehicle control or siControl; **$p < 0.05$ vs. siControl + MCP1.

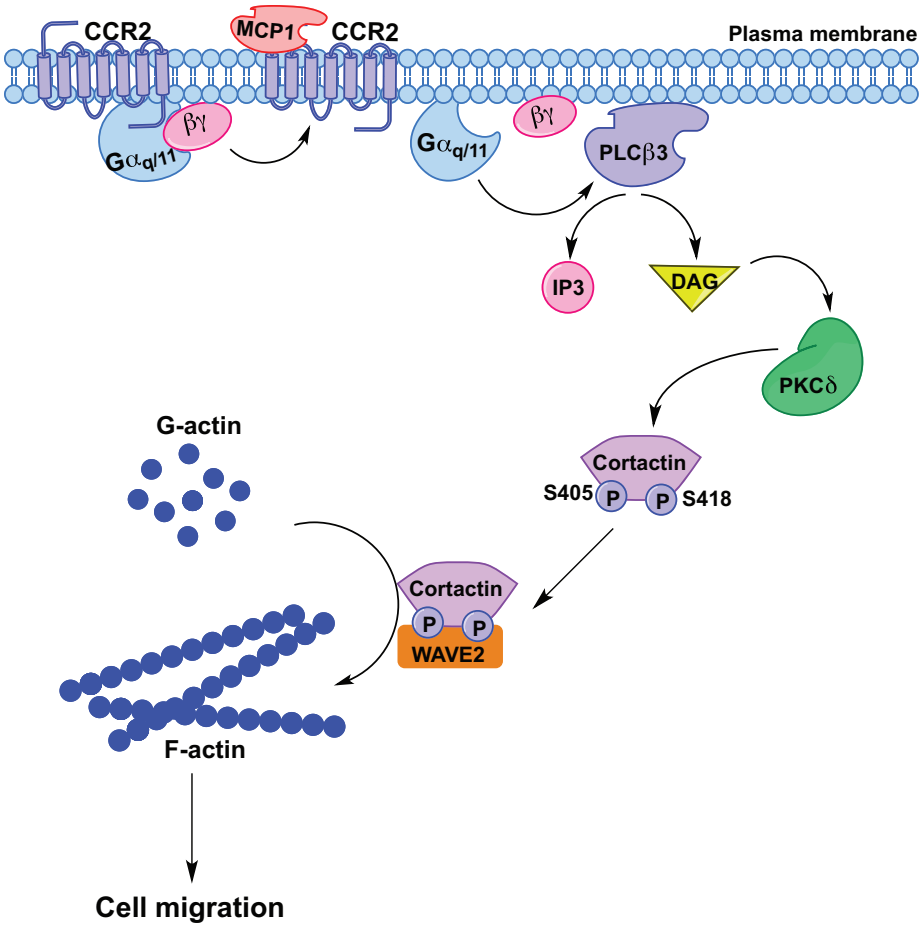

FIGURE 8: Schematic diagram depicting the potential mechanism of cortactin interaction with WAVE2 in mediating MCP1-induced HASMC migration.

The immunocomplexes were released by heating the beads in 40 µl of Laemmli sample buffer and analyzed by Western blotting for the indicated molecules using their specific antibodies.

PLCβ activity assay

PLCglow (WH-15) fluorescent substrate (KXTbio, Chapel Hill, NC) was used to measure PLCβ1-3 activities as described in the manufacturer's instructions. Briefly, cell extracts containing equal amounts of protein from control and various treatments were immunoprecipitated with the indicated PLCβ antibody. The immunocomplexes were suspended in 50 µl of reaction buffer (50 mM 4-(2-hydroxyethyl)-1-piperazineethanesulfonic acid, pH 7.2, 250 mM KCl, 1 mM $CaCl_2$, 2 mM dithiothreitol [DTT], 50 µg/ml BSA, and 0.5% sodium cholate) containing 10 µM WH-15 and incubated for 90 min at room temperature with gentle rocking. The reaction was quenched with the addition of five volumes of 10 mM ethylene glycol tetraacetic acid. After centrifugation at 2000 rpm for 5 min, the supernatant was transferred to a 96-well plate, and the fluorescence intensity was measured using a SpectraMax Gemini XS spectrofluorometer (Molecular Devices, Sunnyvale, CA) at 344-nm excitation and 530-nm emission.

Western blotting

Equal amounts of protein from control and treatment samples were separated by SDS–PAGE and analyzed by Western blotting for the indicated molecules using their specific antibodies, as described previously (Singh *et al.*, 2012). All the primary antibodies were used at 1:500–1:1000 dilutions and incubated overnight at 4°C. Goat anti-rabbit or goat anti-mouse secondary antibodies conjugated with HRP were used at 1:4000–1:5000 dilution. Blots were developed using ECL reagent, and signal intensities were quantified by densitometry using ImageJ software.

G-actin polymerization

Actin polymerization activity was measured by using the Pyrene-Actin Polymerization Kit (Cytoskeleton, Denver, CO) following the manufacturer's instructions. Briefly, cell extracts of control and MCP1-treated cells were immunoprecipitated with anti-cortactin antibody. The cortactin was eluted from the beads with 0.2 M glycine (pH 2.6) and neutralized by the addition of an equal volume of 20 mM Tris-HCl (pH 8.5). To measure actin-polymerization activity, stock pyrene-actin was diluted to 2.3 µM with actin buffer (5 mM Tris-HCl, pH 8.0, and 0.2 mM $CaCl_2$) containing 0.2 mM ATP and 0.5 mM DTT and stored on ice for 60 min to depolymerize the actin oligomers. The actin monomers were collected by centrifugation at 14,000 rpm for 30 min at 4°C. The pyrene-actin monomers were mixed with the eluted cortactin in a 96-well plate containing polymerization buffer (25 mM KCl and 1 mM $MgCl_2$, pH 7.0). The kinetics of actin polymerization was measured by fluorescence intensity generated by the pyrene release for 1 h in a SpectraMax Gemini XS spectrofluorometer at 355/405-nm excitation/emission.

Statistics

All experiments were repeated three times, and the data are presented as mean ± SD. The treatment effects were analyzed by one-way analysis of variance followed by Tukey's post hoc test, and $p < 0.05$ was considered statistically significant.

ACKNOWLEDGMENTS

This work was supported by National Institutes of Health Grants HL069908 and HL103575 to G.N.R.

REFERENCES

Ando K, Obara Y, Sugama J, Kotani A, Koike N, Ohkubo S, Nakahata N (2010). P2Y2 receptor-Gq/11 signaling at lipid rafts is required for UTP-induced cell migration in NG 108-15 cells. J Pharmacol Exp Ther 334, 809–819.

Arai H, Charo IF (1996). Differential regulation of G-protein-mediated signaling by chemokine receptors. J Biol Chem 271, 21814–21819.

Artym VV, Zhang Y, Seillier-Moiseiwitsch F, Yamada KM, Mueller SC (2006). Dynamic interactions of cortactin and membrane type 1 matrix metalloproteinase at invadopodia: defining the stages of invadopodia formation and function. Cancer Res 66, 3034–3043.

Ayala I, Baldassarre M, Giacchetti G, Caldieri G, Tete S, Luini A, Buccione R (2008). Multiple regulatory inputs converge on cortactin to control invadopodia biogenesis and extracellular matrix degradation. J Cell Sci 121, 369–378.

Bach TL, Chen QM, Kerr WT, Wang Y, Lian L, Choi JK, Wu D, Kazanietz MG, Koretzky GA, Zigmond S, *et al.* (2007). Phospholipase cbeta is critical for T cell chemotaxis. J Immunol 179, 2223–2227.

Bajpai AK, Blaskova E, Pakala SB, Zhao T, Glasgow WC, Penn JS, Johnson DA, Rao GN (2007). 15(S)-HETE production in human retinal microvascular

endothelial cells by hypoxia: Novel role for MEK1 in 15(S)-HETE induced angiogenesis. Invest Ophthalmol Vis Sci 48, 4930–4938.
Berk BC (2001). Vascular smooth muscle growth: autocrine growth mechanisms. Physiol Rev 81, 999–1030.
Berridge MJ, Irvine RF (1989). Inositol phosphates and cell signalling. Nature 341, 197–205.
Biber K, Klotz KN, Berger M, Gebicke-Harter PJ, van Calker D (1997). Adenosine A1 receptor-mediated activation of phospholipase C in cultured astrocytes depends on the level of receptor expression. J Neurosci 17, 4956–4964.
Boring L, Gosling J, Cleary M, Charo IF (1998). Decreased lesion formation in CCR2-/- mice reveals a role for chemokines in the initiation of atherosclerosis. Nature 394, 894–897.
Bryce NS, Clark ES, Ja'Mes LL, Currie JD, Webb DJ, Weaver AM (2005). Cortactin promotes cell motility by enhancing lamellipodial persistence. Curr Biol 15, 1276–1285.
Carr MW, Roth SJ, Luther E, Rose SS, Springer TA (1994). Monocyte chemoattractant protein 1 acts as a T-lymphocyte chemoattractant. Proc Natl Acad Sci USA 91, 3652–3656.
Charo IF (1999). CCR2: from cloning to the creation of knockout mice. Chem Immunol 72, 30–41.
Clowes AW, Clowes MM, Fingerle J, Reidy MA (1989). Regulation of smooth muscle cell growth in injured artery. J Cardiovasc Pharmacol 14(Suppl 6), S12–S15.
Craig MJ, Loberg RD (2006). CCL2 (Monocyte Chemoattractant Protein-1) in cancer bone metastases. Cancer Metastasis Rev 25, 611–619.
Deshmane SL, Kremlev S, Amini S, Sawaya BE (2009). Monocyte chemoattractant protein-1 (MCP-1): an overview. J Interferon Cytokine Res 29, 313–326.
Eiseler T, Hausser A, De Kimpe L, Van Lint J, Pfizenmaier K (2010). Protein kinase D controls actin polymerization and cell motility through phosphorylation of cortactin. J Biol Chem 285, 18672–18683.
Gan X, Wang J, Wang C, Sommer E, Kozasa T, Srinivasula S, Alessi D, Offermanns S, Simon MI, Wu D (2012). PRR5L degradation promotes mTORC2-mediated PKC-delta phosphorylation and cell migration downstream of Galpha12. Nat Cell Biol 14, 686–696.
Gerthoffer WT (2007). Mechanisms of vascular smooth muscle cell migration. Circ Res 100, 607–621.
Grassart A, Meas-Yedid V, Dufour A, Olivo-Marin JC, Dautry-Varsat A, Sauvonnet N (2010). Pak1 phosphorylation enhances cortactin-N-WASP interaction in clathrin-caveolin-independent endocytosis. Traffic 11, 1079–1091.
Gu L, Okada Y, Clinton SK, Gerard C, Sukhova GK, Libby P, Rollins BJ (1998). Absence of monocyte chemoattractant protein-1 reduces atherosclerosis in low density lipoprotein receptor-deficient mice. Mol Cell 2, 275–281.
Gu L, Tseng SC, Rollins BJ (1999). Monocyte chemoattractant protein-1. Chem Immunol 72, 7–29.
Helgeson LA, Nolen BJ (2013). Mechanism of synergistic activation of Arp2/3 complex by cortactin and N-WASP. Elife 2, e00884.
Huang W, Hicks SN, Sondek J, Zhang Q (2011). A fluorogenic, small molecule reporter for mammalian phospholipase C isozymes. ACS Chem Biol 6, 223–228.
Huang C, Liu J, Haudenschild CC, Zhan X (1998). The role of tyrosine phosphorylation of cortactin in the locomotion of endothelial cells. J Biol Chem 273, 25770–25776.
Iwabu A, Smith K, Allen FD, Lauffenburger DA, Wells A (2004). Epidermal growth factor induces fibroblast contractility and motility via a protein kinase C delta-dependent pathway. J Biol Chem 279, 14551–14560.
Kamiya K, Ryer E, Sakakibara K, Zohlman A, Kent KC, Liu B (2007). Protein kinase C delta activated adhesion regulates vascular smooth muscle cell migration. J Surg Res 141, 91–96.
Kelley GG, Kaproth-Joslin KA, Reks SE, Smrcka AV, Wojcikiewicz RJ (2006). G-protein-coupled receptor agonists activate endogenous phospholipase Cepsilon and phospholipase Cbeta3 in a temporally distinct manner. J Biol Chem 281, 2639–2648.
Kelley LC, Hayes KE, Ammer AG, Martin KH, Weed SA (2010). Cortactin phosphorylated by ERK1/2 localizes to sites of dynamic actin regulation and is required for carcinoma lamellipodia persistence. PLoS One 5, e13847.
Kinley AW, Weed SA, Weaver AM, Karginov AV, Bissonette E, Cooper JA, Parsons JT (2003). Cortactin interacts with WIP in regulating Arp2/3 activation and membrane protrusion. Curr Biol 13, 384–393.
Kruchten AE, Krueger EW, Wang Y, McNiven MA (2008). Distinct phosphoforms of cortactin differentially regulate actin polymerization and focal adhesions. Am J Physiol Cell Physiol 295, C1113–C1122.
Kuang Y, Wu Y, Jiang H, Wu D (1996). Selective G protein coupling by C-C chemokine receptors. J Biol Chem 271, 3975–3978.
Kundumani-Sridharan V, Singh NK, Kumar S, Gadepalli R, Rao GN (2013). Nuclear factor of activated T cells c1 mediates p21-activated kinase 1 activation in the modulation of chemokine-induced human aortic smooth muscle cell F-actin stress fiber formation, migration, and proliferation and injury-induced vascular wall remodeling. J Biol Chem 288, 22150–22162.
Lee JS, Yang EJ, Kim IS (2009). The roles of MCP-1 and protein kinase C delta activation in human eosinophilic leukemia EoL-1 cells. Cytokine 48, 186–195.
Lefevre S, Knedla A, Tennie C, Kampmann A, Wunrau C, Dinser R, Korb A, Schnäker EM, Tarner IH, Robbins PD, *et al.* (2009). Synovial fibroblasts spread rheumatoid arthritis to unaffected joints. Nat Med 15, U1414–U1410.
Li C, Wernig F, Leitges M, Hu Y, Xu Q (2003). Mechanical stress-activated PKCdelta regulates smooth muscle cell migration. FASEB J 17, 2106–2108.
Li Z, Jiang H, Xie W, Zhang Z, Smrcka AV, Wu D (2000). Roles of PLC-beta2 and -beta3 and PI3Kgamma in chemoattractant-mediated signal transduction. Science 287, 1046–1049.
Llado A, Timpson P, Vila de Muga S, Moreto J, Pol A, Grewal T, Daly RJ, Enrich C, Tebar F (2008). Protein kinase Cdelta and calmodulin regulate epidermal growth factor receptor recycling from early endosomes through Arp2/3 complex and cortactin. Mol Biol Cell 19, 17–29.
Lyon AM, Dutta S, Boguth CA, Skiniotis G, Tesmer JJ (2013). Full-length Galpha(q)-phospholipase C-beta3 structure reveals interfaces of the C-terminal coiled-coil domain. Nat Struct Mol Biol 20, 355–362.
Lyon AM, Taylor VG, Tesmer JJ (2014). Strike a pose: Galphaq complexes at the membrane. Trends Pharmacol Sci 35, 23–30.
MacGrath SM, Koleske AJ (2012). Cortactin in cell migration and cancer at a glance. J Cell Sci 125, 1621–1626.
Martinez-Quiles N, Ho H-YH, Kirschner MW, Ramesh N, Geha RS (2004). Erk/Src phosphorylation of cortactin acts as a switch on-switch off mechanism that controls its ability to activate N-WASP. Mol Cell Biol 24, 5269–5280.
Matsumura M, Tanaka N, Kuroki T, Ichihashi M, Ohba M (2003). The eta isoform of protein kinase C inhibits UV-induced activation of caspase-3 in normal human keratinocytes. Biochem Biophys Res Commun 303, 350–356.
Mellor H, Parker PJ (1998). The extended protein kinase C superfamily. Biochem J 332, 281–292.
Miki H, Sasaki T, Takai Y, Takenawa T (1998a). Induction of filopodium formation by a WASP-related actin-depolymerizing protein N-WASP. Nature 391, 93–96.
Miki H, Suetsugu S, Takenawa T (1998b). WAVE, a novel WASP-family protein involved in actin reorganization induced by Rac. EMBO J 17, 6932–6941.
Mitchison TJ, Cramer LP (1996). Actin-based cell motility and cell locomotion. Cell 84, 371–379.
Mullins RD, Pollard TD (1999). Structure and function of the Arp2/3 complex. Curr Opin Struct Biol 9, 244–249.
Østerud B, Bjørklid E (2003). Role of monocytes in atherogenesis. Physiol Rev 83, 1069–1112.
Potula HS, Wang D, Quyen DV, Singh NK, Kundumani-Sridharan V, Karpurapu M, Park EA, Glasgow WC, Rao GN (2009). Src-dependent STAT-3-mediated expression of monocyte chemoattractant protein-1 is required for 15(S)-hydroxyeicosatetraenoic acid-induced vascular smooth muscle cell migration. J Biol Chem 284, 31142–31155.
Roque M, Kim WJ, Gazdoin M, Malik A, Reis ED, Fallon JT, Badimon JJ, Charo IF, Taubman MB (2002). CCR2 deficiency decreases intimal hyperplasia after arterial injury. Arterioscler Thromb Vasc Biol 22, 554–559.
Schober A, Zernecke A, Liehn EA, von Hundelshausen P, Knarren S, Kuziel WA, Weber C (2004). Crucial role of the CCL2/CCR2 axis in neointimal hyperplasia after arterial injury in hyperlipidemic mice involves early monocyte recruitment and CCL2 presentation on platelets. Circ Res 95, 1125–1133.
Si Y, Ren J, Wang P, Rateri DL, Daugherty A, Shi XD, Kent KC, Liu B (2012). Protein kinase C-delta mediates adventitial cell migration through regulation of monocyte chemoattractant protein-1 expression in a rat angioplasty model. Arterioscler Thromb Vasc Biol 32, 943–954.
Singh NK, Kotla S, Dyukova E, Traylor JG Jr, Orr AW, Chernoff J, Marion TN, Rao GN (2015). Disruption of p21-activated kinase 1 gene diminishes atherosclerosis in apolipoprotein E-deficient mice. Nat Commun 6, 7450.
Singh NK, Kundumani-Sridharan V, Kumar S, Verma SK, Kotla S, Mukai H, Heckle MR, Rao GN (2012). Protein kinase N1 is a novel substrate

of NFATc1-mediated cyclin D1-CDK6 activity and modulates vascular smooth muscle cell division and migration leading to inward blood vessel wall remodeling. J Biol Chem 287, 36291–36304.
Singh NK, Wang D, Kundumani-Sridharan V, Quyen DV, Niu J, Rao GN (2011). 15-Lipoxygenase-1-enhanced Src-Janus kinase 2-signal transducer and activator of transcription 3 stimulation and monocyte chemoattractant protein-1 expression require redox-sensitive activation of epidermal growth factor receptor in vascular wall remodeling. J Biol Chem 286, 22478–22488.
Smrcka AV, Sternweis PC (1993). Regulation of purified subtypes of phosphatidylinositol-specific phospholipase C beta by G protein alpha and beta gamma subunits. J Biol Chem 268, 9667–9674.
Stupack DG, Cho SY, Klemke RL (2000). Molecular signaling mechanisms of cell migration and invasion. Immunol Res 21, 83–88.
Suetsugu S, Miki H, Yamaguchi H, Obinata T, Takenawa T (2001). Enhancement of branching efficiency by the actin filament-binding activity of N-WASP/WAVE2. J Cell Sci 114, 4533–4542.
Takahashi K, Suzuki K (2009). Membrane transport of WAVE2 and lamellipodia formation require Pak1 that mediates phosphorylation and recruitment of stathmin/Op18 to Pak1-WAVE2-kinesin complex. Cell Signal 21, 695–703.
Uruno T, Liu J, Zhang P, Fan Y-x, Egile C, Li R, Mueller SC, Zhan X (2001). Activation of Arp2/3 complex-mediated actin polymerization by cortactin. Nat Cell Biol 3, 259–266.
Vicente-Manzanares M, Webb DJ, Horwitz AR (2005). Cell migration at a glance. J Cell Sci 118, 4917–4919.
Wang W, Liu Y, Liao K (2011). Tyrosine phosphorylation of cortactin by the FAK-Src complex at focal adhesions regulates cell motility. BMC Cell Biol 12, 49.
Weaver AM, Karginov AV, Kinley AW, Weed SA, Li Y, Parsons JT, Cooper JA (2001). Cortactin promotes and stabilizes Arp2/3-induced actin filament network formation. Curr Biol 11, 370–374.
Webb BA, Zhou S, Eves R, Shen L, Jia L, Mak AS (2006). Phosphorylation of cortactin by p21-activated kinase. Arch Biochem Biophys 456, 183–193.
Weed SA, Karginov AV, Schafer DA, Weaver AM, Kinley AW, Cooper JA, Parsons JT (2000). Cortactin localization to sites of actin assembly in lamellipodia requires interactions with F-actin and the Arp2/3 complex. J Cell Biol 151, 29–40.
Wu H, Reynolds AB, Kanner SB, Vines RR, Parsons JT (1991). Identification and characterization of a novel cytoskeleton-associated pp60src substrate. Mol Cell Biol 11, 5113–5124.
Xu L, Warren M, Rose W, Gong W, Wang J (1996). Human recombinant monocyte chemotactic protein and other CC chemokines bind and induce directional migration of dendritic cells in vitro. J Leukoc Biol 60, 365–371.
Yamaguchi H, Condeelis J (2007). Regulation of the actin cytoskeleton in cancer cell migration and invasion. Biochim Biophys Acta 1773, 642–652.
Yamaguchi H, Wyckoff J, Condeelis J (2005). Cell migration in tumors. Curr Opin Cell Biol 17, 559–564.
Yamazaki D, Suetsugu S, Miki H, Kataoka Y, Nishikawa S, Fujiwara T, Yoshida N, Takenawa T (2003). WAVE2 is required for directed cell migration and cardiovascular development. Nature 424, 452–456.
Zeng H, Zhao D, Mukhopadhyay D (2002). KDR stimulates endothelial cell migration through heterotrimeric G protein Gq/11-mediated activation of a small GTPase RhoA. J Biol Chem 277, 46791–46798.
Zhang X, Yuan Z, Zhang Y, Yong S, Salas-Burgos A, Koomen J, Olashaw N, Parsons JT, Yang XJ, Dent SR, *et al.* (2007). HDAC6 modulates cell motility by altering the acetylation level of cortactin. Mol Cell 27, 197–213.
Zhang Y, Zhang M, Dong H, Yong S, Li X, Olashaw N, Kruk PA, Cheng JQ, Bai W, Chen J, *et al.* (2009). Deacetylation of cortactin by SIRT1 promotes cell migration. Oncogene 28, 445–460.